117: Synoptic and Orographic Control of Observed Drop Size Distributions during the OLYMPEX Field Campaign

Joseph P. Zagrodnik, Lynn McMurdie, Robert A. Houze, Jr., University of Washington

Introduction and OLYMPEX Overview

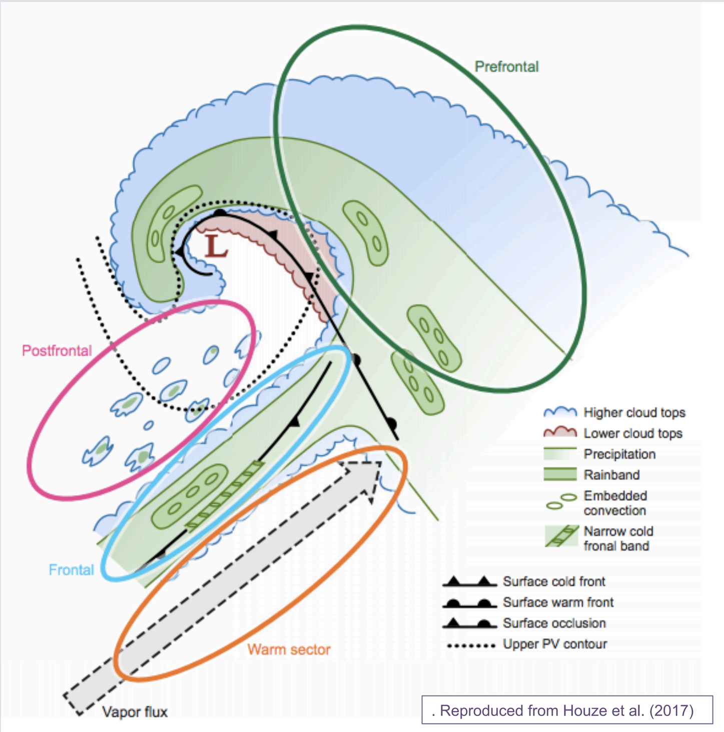

Landfalling extratropical cyclones on the west coast of continents are important because of:

- Copious precipitation production from interactions with coastal mountains
- Hazards such as flooding and landslides
- Snow pack for summer water supply

The 2015-16 OLYMPEX field campaign:

- Ground validation for GPM satellite
- Modification of frontal systems as they pass over coastal mountains
- Extensive observational assets:
  - Four NASA aircraft
  - Four dual-polarization radars
  - Ground instruments measuring particle sizes at a variety of elevations
  - High elevation snow pack measurements

Objectives of this study:

- Combine ground-based DSD measurements with synoptic and radar data
- Focus on periods of stratiform rain
- Determine mechanisms responsible for the modification and enhancement of precipitation on the windward slopes of coastal mountains

Past studies have shown that maritime frontal cyclones have 4 characteristic regimes:

- Prefrontal: leading edge of precipitation, warm advection, rising melting levels
- Frontal: broad elongated cloud shield with banded precipitation
- Warm sector: contains a narrow filament of water vapor flux (atmospheric river)
- Postfrontal: cold, small-scale convective features

Site Locations and Data Processing

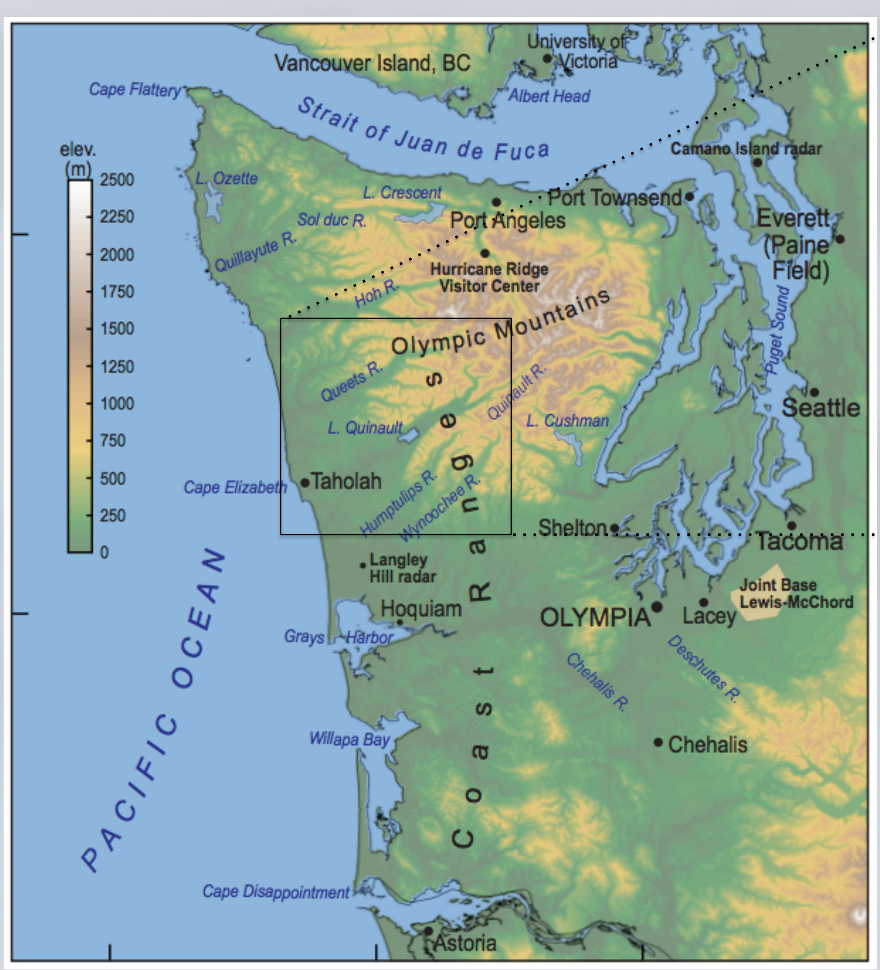

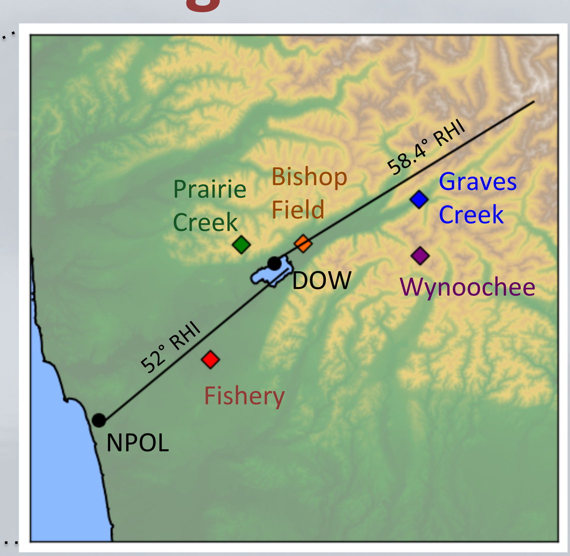

Ground Site	Elevation (m)	Description
Fishery	52	Upstream, low-elevation
Bishop Field	85	Front of valley, low-elevation
Prairie Creek	543	Front of valley, mid-elevation
Graves Creek	180	Interior valley, low-elevation
Wynoochee	1020	Interior high-elevation

Data processing for statistical section:

- 3-h synoptic data from NARR reanalysis
- Rain gauge, Pluvio-400 and Parsivel[2] disdrometer data organized into 3-h periods centered on synoptic times
- QC removed the following periods:
  - All postfrontal periods removed (only stratiform precipitation is considered)
  - Snow/ice (Tipping bucket gauges and Parsivel)
  - Condensation/splashing on Parsivel optics
  - Minimum precipitation rate: 1 mm h^{-1}

N_w-D_0 Methodology:

Comparing DSDs from different time periods requires the use of a normalized DSD (Testud et al. 2001):

$$N_w = \frac{3.67^4 10^3 LWC}{\pi \rho_w D_0^4}$$

D_0: median drop diameter (mm)
N_w: Normalized intercept paramete (mm^{-3} m^{-1})
LWC: liquid water content measured by Parsivel[2]

Interpretation:
Unlike the intercept in a gamma DSD, N_w does not depend on DSD shape. So the relative number and size of drops in different DSDs can be described by the interplay between N_w and D_0.

DOW on Lake Quinault

Graves Creek Parsivel and Gauges

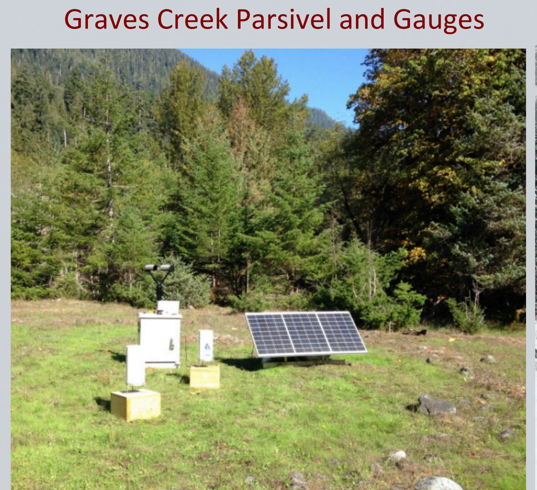

High-elevation Wynoochee Site

Case Study: 12-13 November 2015

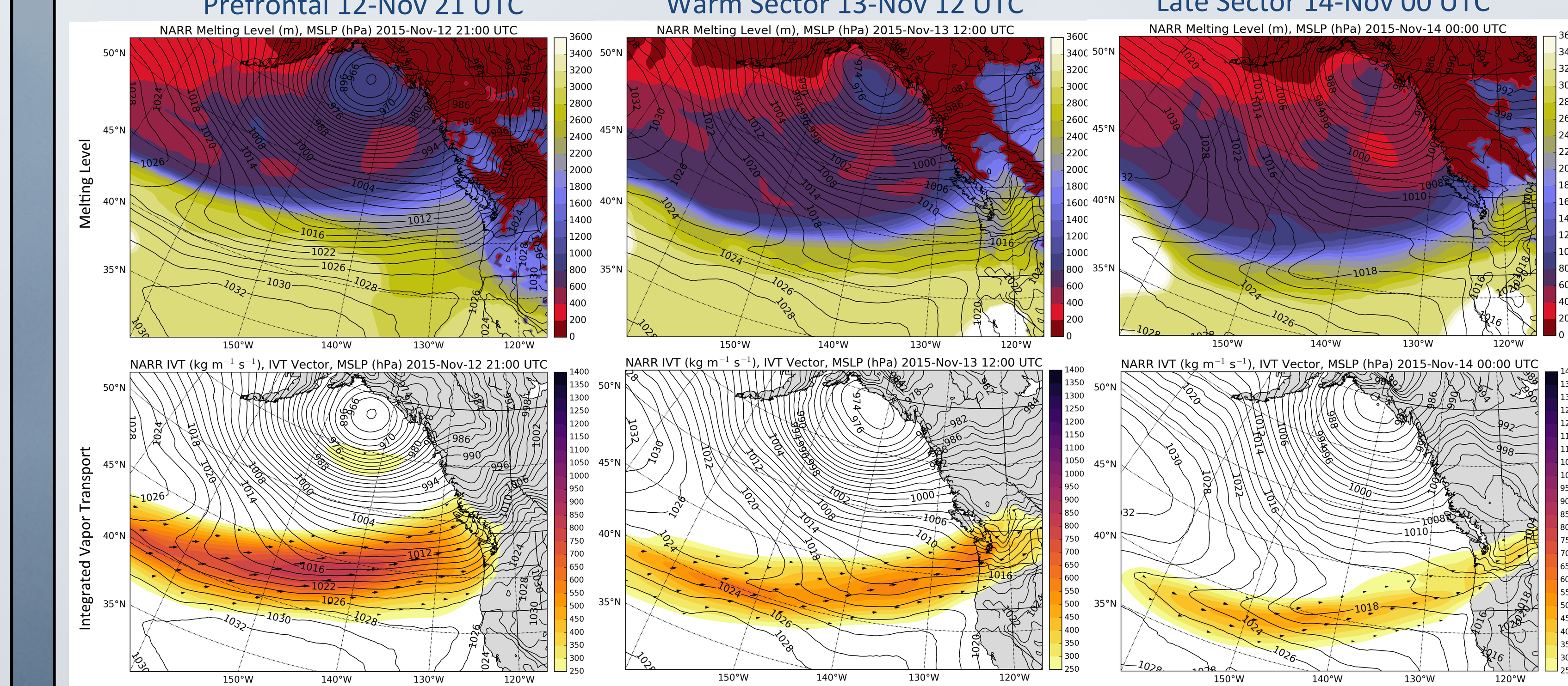

Upstream of Olympic Mountains:

Melting Level:

Prefrontal: Rises from 1500 m to 2600 m

Warm Sector: Steady at 2600 m

Late Sector: Remains above 2000 m until end of precipitation

Vapor Transport:

Prefrontal: Increases from 250 to 480 kg m^{-1} s^{-1}

Warm Sector: Ranges between 400-600 kg m^{-1} s^{-1}

Late Sector: Slowly decreases from 400 to 250 kg m^{-1} s^{-1}

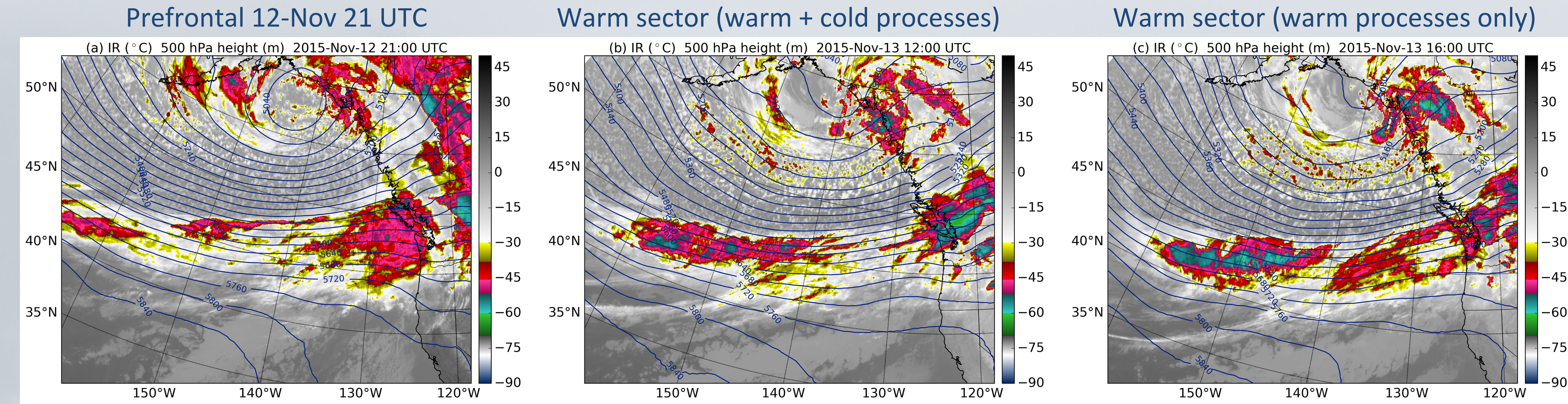

A warm, intense Atmospheric River type system passed over the Olympic Peninsula on 12-13 Nov 2015. It produced over 370 mm of rain (14.5 inches) of rain at Prairie Creek with lesser amounts upstream, in the interior valley, and at high elevations. The precipitation enhancement pattern and Prairie Creek DSDs co-evolved following the synoptic evolution of the storm.

Prefrontal period (blue circles):

The DSD was initially close to the most frequent distribution (small quantities of small and large drops). As the warm front approached aloft, large drops increased first (12-Nov 18 UTC), followed by small to medium drops around 12-Nov 22 UTC. The rain rate at Prairie Creek

Warm sector with warm processes dominating (yellow diamonds):

Most of the warm sector had DSDs in the 'heavy rain' regime with high values of N_w indicating the production of large quantities of small to medium sized drops by warm processes (condensation + collision-coalescence).

Warm sector with both warm and cold processes (red squares):

A frontal wave within the warm sector passed through the sites on 13-Nov 10-14 UTC (see satellite), temporarily reducing N_w and increasing D_0. Surprisingly this had little effect on the Prairie Creek rain rates, suggesting the warm processes are not dependent on 'seeder' drops formed by melting.

Late sector (orange triangles):

Warm, moist flow continued for several hours after the cold front. Large quantities of < 1 mm drops continued to fall at Prairie Creek.

Prairie Creek 1-hour DSDs

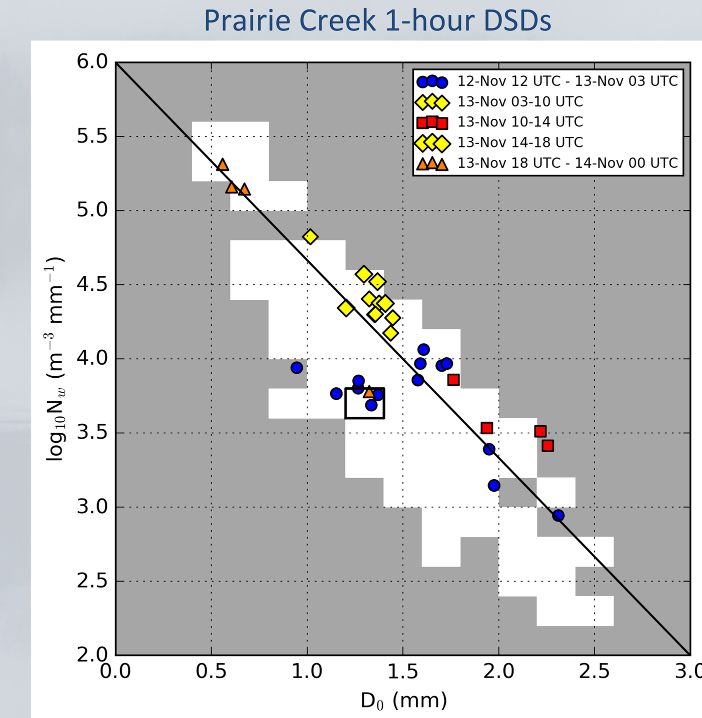

Precipitation Rate and DSD Time Series

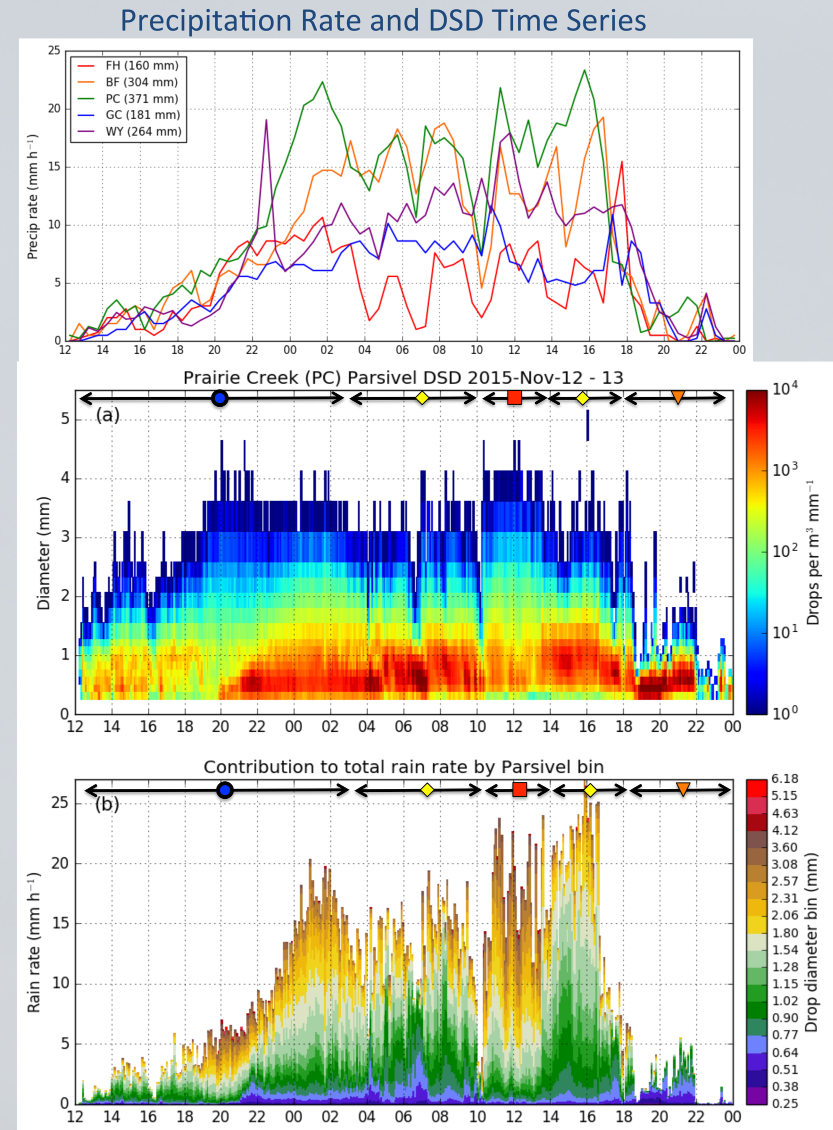

NPOL+DOW combined RHI sectors:

Reflectivity (left column):

- Large drops = high echo top, strong bright band (12-Nov 12:52 UTC and 13-Nov 11:52 UTC)
- Small drops = low echo top, weak bright band, low-level enhancement below 1 km (13-Nov 11:52 and 15:52 UTC)

Radial Velocity (right column):

- Large drops = low-level jet lifting through/above bright band
- Small drops = low-level jet lifts below bright band

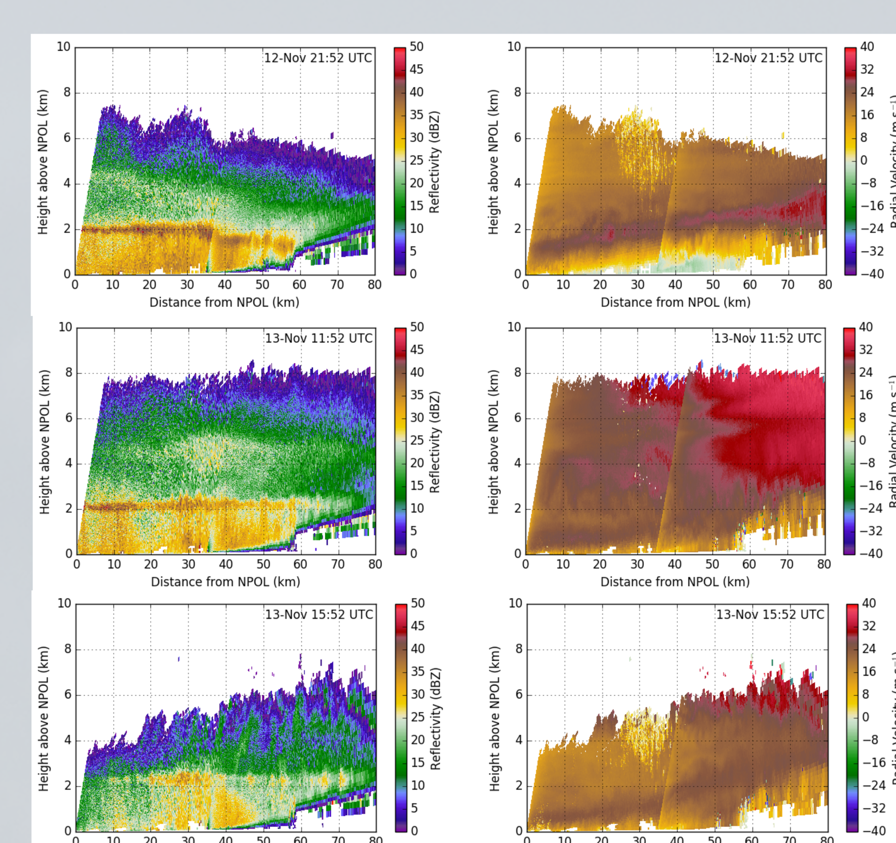

Full Cold Season Stratiform Rain Statistics

N_w-D_0 Distribution (top) and Rain Rate (bottom)

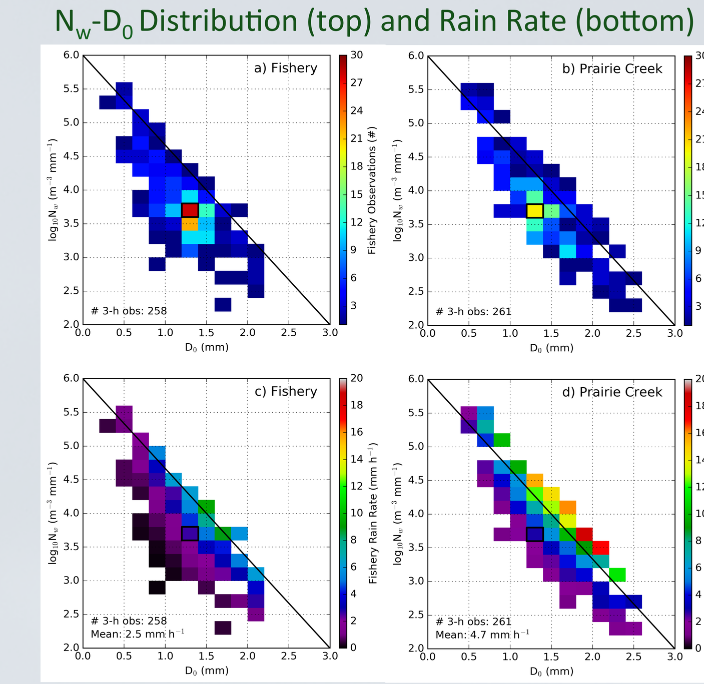

All of the plots in this section show the 3-h disdrometer data binned into 2D-histograms by median drop diameter (D_0) and normalized intercept parameter (N_w).

Compared with the upstream site (Fishery), the mid-elevation site (Prairie Creek) has:

- The most-frequent DSD in the same location.
- More outliers, especially in DSD bins that produce rain rates > 10 mm h^{-1}.
- A greater variation of N_w-D_0 combinations, meaning the DSD is more variable at Prairie Creek.

Difference in Rain Rate Relative to Prairie Creek

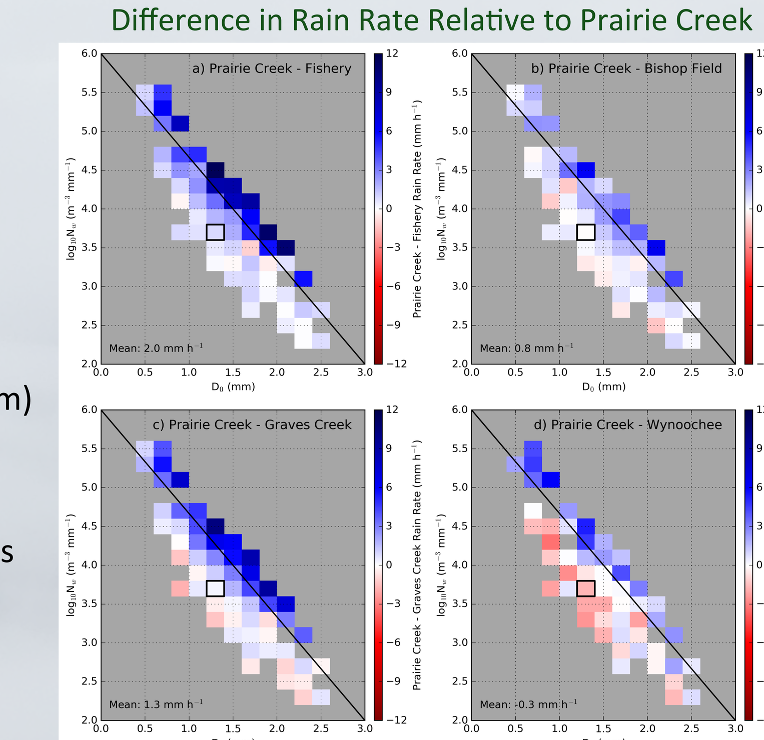

The Prairie Creek DSDs fall into four different regimes that are each associated with a unique synoptic environment and precipitation enhancement pattern:

1. Low N_w, Low D_0 (Most Frequent Distribution):
   - Climatologically average melting level (~1800 m)
   - IVT: 250-300 kg m^{-1} s^{-1}
   - Low levels: static stability, southerly flow
   - Modest precip enhancement at high elevations
2. High N_w, Low D_0 (Large quantities of small drops):
   - High melting level (> 2000 m)
   - IVT: 300-400 kg m^{-1} s^{-1}
   - Low-levels: static stability, westerly flow
   - Not convective
   - Precip enhanced at low-to-mid elevations
3. Low N_w, High D_0 (Small quantities of large drops):
   - Low melting level (< 1500 m), weak IVT
   - Flow generally southerly, sometimes from west or northwest
   - Conditional instability
   - Negligible precip enhancement
4. High N_w, High D_0 (Heavy Rain):
   - High melting level (> 2000 m)
   - Very high IVT (400 – 800 kg m^{-1} s^{-1})
   - Strong low-level flow from the west-southwest
   - Moist-neutral stability
   - Extreme precip enhancement, especially at low-to-mid elevations near the front of the topographic barrier
   - Modest precip enhancement at high elevations
   - Includes Atmospheric River type storms

Synoptic Environment and Low-Level Stability

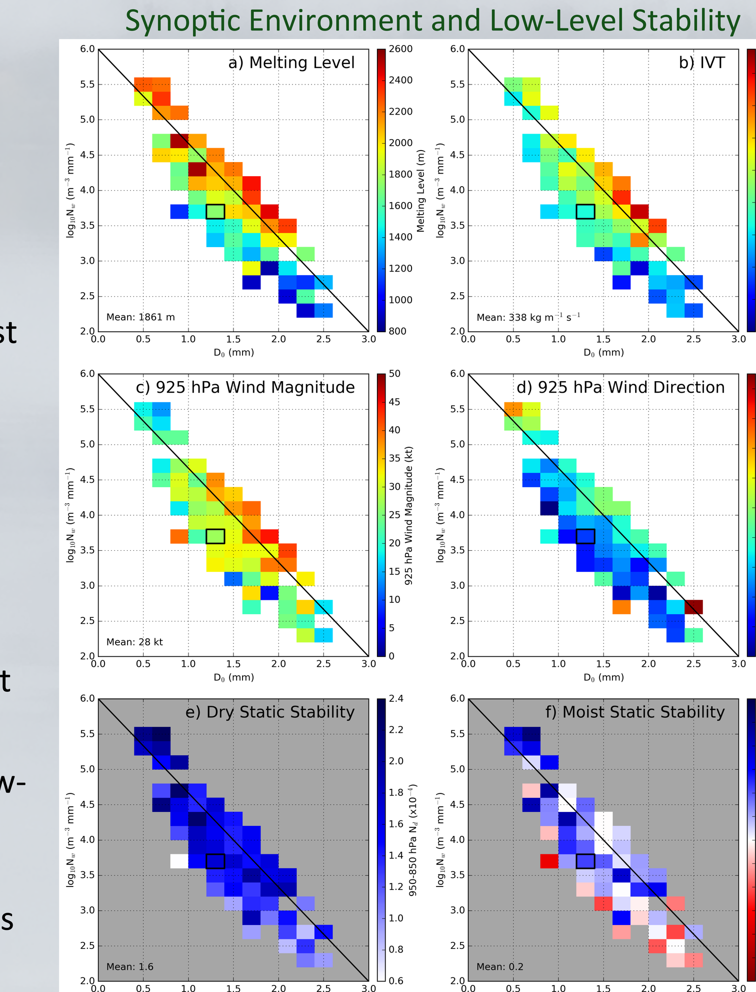

Conclusions

The combination of the statistical distribution and case study reveal the following properties of cold-season DSDs:

- Four DSD regimes emerge based on the relative contribution of small and large drops to the total rainfall.
- Transitions between DSD regimes are closely related to the large-scale synoptic environment (flow, temp. stability).
- The most frequent DSD contains modest drop concentrations, a climatologically average environment, and slight precipitation enhancement at high elevations.
- The greatest precipitation enhancement occurs via small-to-medium sized drops in the warm sector at low-to-mid elevations. It is associated with a high melting level, high IVT, a west-southwest low-level jet, and moist-neutral stability.

Location of the Four DSD Regimes

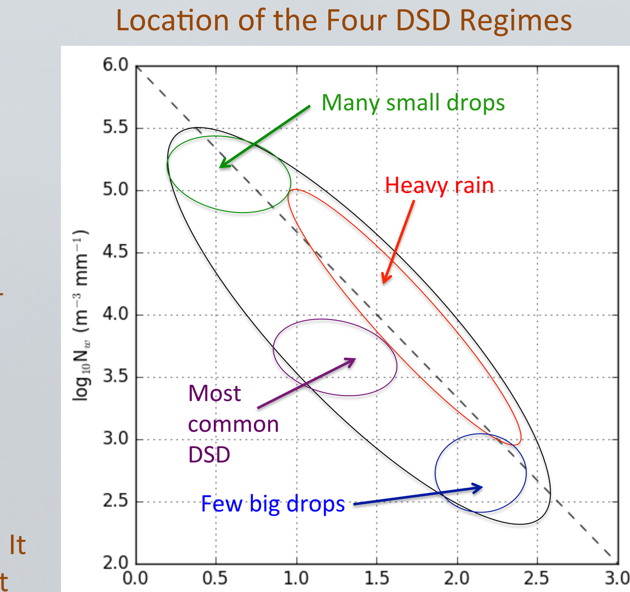

Acknowledgements

This work was supported through NASA grants NNX15AL38G, NNX16AK05G, and NNX16AD75G and NSF Grand AGS-1503155. The authors would like to thank M. Wingo, B. Baccus, C. Urnes, R. A. Hart, N. Johnson, S. Domokos, H. Mohrmann, B. Jameson, B. Gilles, and J. Nowak for making major contributions to deployment and maintenance of the ground sites used in this study. A. Tokay, P. Gatlin, and D. Wolff helped process and interpret disdrometer data .